

# Mechanism and Kinetics of RAFT-Mediated Graft Polymerization of Styrene on a Solid Surface. 1. Experimental Evidence of Surface Radical Migration

Yoshinobu Tsujii, Muhammad Ejaz, Koichi Sato, Atsushi Goto, and Takeshi Fukuda\*

*Institute for Chemical Research, Kyoto University, Uji, Kyoto 611-0011, Japan*

*Received April 27, 2001*

**ABSTRACT:** The mechanism and kinetics of RAFT-mediated graft polymerization of styrene initiated on a silica particle were studied, where RAFT is the reversible addition–fragmentation chain transfer (RAFT) process. To prepare probe graft polymers with a dithiobenzoyl (X) group at the chain end, oligomeric polystyrene (PS) was grafted on a silica particle by the surface-initiated atom transfer radical polymerization (ATRP) technique, and then the terminal halogen atom of the graft polymer was converted to the X group by the reaction with 1-phenylethyl dithiobenzoate in the presence of CuBr/dHbipy complex in toluene. The graft polymerization of styrene on the PS–X-grafted silica particle was carried out in the presence of a free RAFT agent. After the polymerization, the graft chain was cleaved from the silica particle by treatment with HF and characterized. The GPC analysis revealed that the graft polymers, while their  $M_n$  increased linearly with increasing monomer conversion, gave a GPC curve with a prominent shoulder assignable to the recombined (dead) polymer. It was proved that the enhanced recombination is specific to the RAFT-mediated graft polymerization and is due to the effective migration of radical on the surface by sequential degenerative (exchange) chain transfer. This is a kind of reaction–diffusion process.

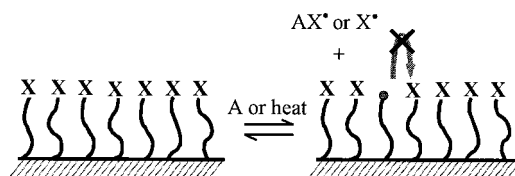
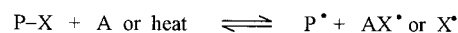
## Introduction

Living radical polymerization is a new and robust method to synthesize well-defined polymers and copolymers with low polydispersity. It includes nitroxide-mediated polymerization (NMP),<sup>1–7</sup> atom transfer radical polymerization (ATRP),<sup>8–12</sup> and RAFT-mediated polymerization (RAFT-MP),<sup>13–16</sup> where RAFT stands for reversible addition–fragmentation chain transfer. All members of living radical polymerization are commonly characterized by a reversible activation reaction of potentially active or “dormant” species.<sup>17</sup> In NMP, the dormant chain P–X is reversibly dissociated into a growing radical P• and a stable (nitroxyl) radical X•. In ATRP, the P–X bond, where X is a halogen like Cl or Br, is reversibly cleaved by a catalytic action of an activator A, producing P• and a complex AX•, where the deactivator AX• plays the role of a stable radical in NMP. RAFT-MP is mechanistically different from NMP and ATRP. A RAFT process is a kind of degenerative chain transfer reaction, in which activation and deactivation occur at the same time or an active site migrates from one chain to another.

Recently, some living radical polymerization techniques were applied to surface-initiated graft polymerization.<sup>18–25</sup> Using ATRP, we successfully grafted a low-polydispersity polymer on a solid surface with the highest-ever reported graft density.<sup>18</sup> ATRP was applicable to various substrates such as silicon wafer, silica particle, and porous glass filter.<sup>18</sup>

This paper reports the first application of RAFT-MP to surface-initiated graft polymerization. Unlike in an ATRP or a NMP system, a graft-polymer radical in a RAFT system may undergo a RAFT process with a

### (a) ATRP or NMP



### (b) RAFT

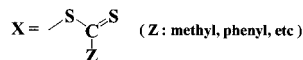
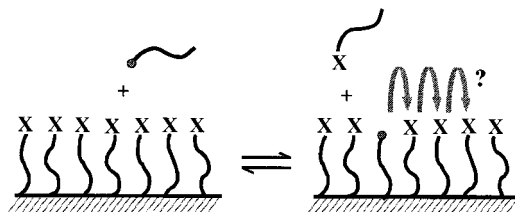
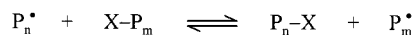


**Figure 1.** Comparison of the key processes in (a) the ATRP- or NMP-mediated and (b) RAFT-mediated graft polymerizations.

neighboring graft polymer as well as with a free polymer (Figure 1). We previously observed for the surface-initiated ATRP that all of the graft polymers more or less simultaneously grow, maintaining an extremely high graft density so that the graft chains are highly stretched in a good solvent.<sup>26</sup> This suggests that the

\* To whom correspondence should be addressed: e-mail fukuda@scl.kyoto-u.ac.jp.

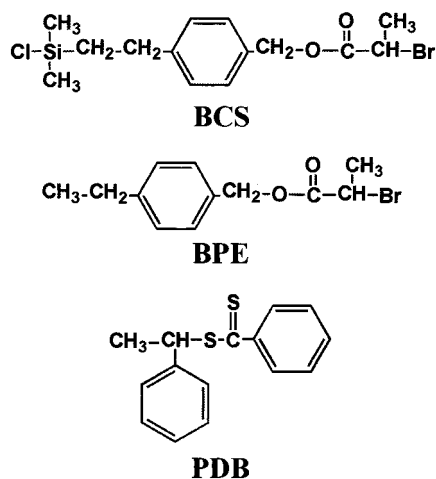


**Figure 2.** Chemical structures of BCS, BPE, and PDB.

chain ends of these graft polymers are highly localized or concentrated near the free surface of the graft layer.<sup>27,28</sup> In the RAFT system, therefore, chain transfer should be unusually effective among the graft polymers. Degenerative chain transfer reactions occurring in sequence are viewed as a migration or reaction–diffusion process of the otherwise severely localized graft radicals. A central issue in this paper is to present experimental evidence showing that the graft radicals do migrate in the RAFT-MP of styrene on a silica particle.

## Experimental Section

**Materials.** The silica particle used was Aerosil 200CF (Nippon Aerosil Co., Japan). The BET-estimated surface area, particle diameter, and silanol content were  $200 \pm 25$  m<sup>2</sup>/g, 12 nm, and 1.37 mmol/g, respectively. Styrene (Nacalai Tesque Inc., Japan) was purified by the standard method. A ligand, 4,4′-di-*n*-heptyl-2,2′-bipyridine (dHbipy), and a RAFT agent, 1-phenylethyl dithiobenzoate (PDB, see Figure 2), were prepared according to the methods reported by Matyjaszewski et al.<sup>29</sup> and Moad et al.,<sup>13</sup> respectively. Toluene was distilled over CaH<sub>2</sub>. Unless otherwise specified, all other reagents were purchased from commercially available sources and used as received.

**Synthesis of ATRP Initiators.** The surface-immobilizable ATRP initiator, 2-(4-(2-bromopropionyloxymethylphenyl)-ethyl)dimethylchlorosilane (BCS, see Figure 2), was synthesized by the reaction of 4-vinylbenzyl alcohol (Seimi Chemical Co., Ltd., Japan, 99.5% of purity) with 2-bromopropionyl bromide followed by hydrosilylation with dimethylchlorosilane. To 150 mL of THF solution containing 4-vinylbenzyl alcohol (10.4 g, 78 mmol) and triethylamine (10.8 mL, 78 mmol), 2-bromopropionyl bromide (8.2 mL, 78 mmol) was added dropwise at 0 °C. The solution was allowed to be stirred for 2 h at 0 °C and for another 2 h at room temperature. The reactant was washed with an aqueous NaHCO<sub>3</sub> (saturated) solution and extracted three times with 200 mL of CHCl<sub>3</sub>. The extracted solution was dried over anhydrous Na<sub>2</sub>SO<sub>4</sub>, and the solvent was evaporated off. Thus obtained crude product was purified by silica gel column chromatography using a mixture of hexane and ethyl acetate (9:1 by volume) as eluent, giving 4-vinylbenzyl 2-bromopropionate (VBP) as a colorless oil. Hydrosilylation was carried out by adding dimethylchlorosilane (25 g) to VBP (5 g, 18.6 mmol) dropwise in the presence of 40 mg of chloroplatinic acid (0.5 mL of 1:1 ethanol/diethyl ether solution) as a catalyst and refluxing the mixture for 3 h. After an excess of dimethylchlorosilane was removed by vacuum distillation, the oily residue was diluted with 20 mL of dry

dichloromethane and passed through a short column of anhydrous Na<sub>2</sub>SO<sub>4</sub> to remove the catalyst. Thus obtained dichloromethane solution of BCS (about 20 wt %) was used without further purification. <sup>1</sup>H NMR (CDCl<sub>3</sub>):  $\delta$  0.2–0.5 (6H, Si–CH<sub>3</sub>), 1.1–1.2 (2H, Si–CH<sub>2</sub>), 1.8–1.9 (3H, CHBr–CH<sub>3</sub>), 2.7–2.8 (2H, Ph–CH<sub>2</sub>–CH<sub>2</sub>), 4.3–4.4 (1H, CHBr), 5.1–5.2 (2H, CH<sub>2</sub>–O), 7.1–7.4 (4H, aromatic).

The model (free) ATRP initiator, (4-(2-bromopropionyloxymethylphenyl)ethane (BPE, see Figure 2), was synthesized by the esterification of 4-ethylbenzyl alcohol with 2-bromopropionyl bromide according to the same procedure as VBP except that 4-ethylbenzyl alcohol (10.5 g, 78 mmol) was used in place of 4-vinylbenzyl alcohol. <sup>1</sup>H NMR (CDCl<sub>3</sub>):  $\delta$  1.2–1.3 (3H, CH<sub>2</sub>–CH<sub>3</sub>), 1.8–1.9 (3H, CHBr–CH<sub>3</sub>), 2.7–2.8 (2H, Ph–CH<sub>2</sub>–CH<sub>3</sub>), 4.3–4.4 (1H, CHBr), 5.1–5.2 (2H, CH<sub>2</sub>–O), 7.1–7.4 (4H, aromatic).

**Preparation of Precursory Graft Polymer with a Terminal RAFT Moiety.** BCS was immobilized on the silica particle by chemisorption: silica particles (4.5 g), which had been dried overnight in a vacuum at 110 °C before use, were suspended and stirred in 200 mL of dry toluene containing BCS (10 mL of dichloromethane solution) and triethylamine (4.5 mL) for 24 h at room temperature. The modified silica particles were purified by successive dispersion–centrifugation processes using toluene, ethanol, water, and then diethyl ether to completely remove unimmobilized initiator and other impurities. The obtained white solid was dried overnight in a vacuum.

The modified silica particles (0.90 g) were dispersed by ultrasonication in degassed styrene (36 g) containing CuBr (0.25 g, 1.7 mmol), dHbipy (1.23 g, 3.5 mmol), and BPE (0.50 g, 1.8 mmol) as a free ATRP initiator. The free initiator was added to control the polymerization.<sup>18,21,22</sup> After the ATRP graft polymerization at 110 °C for 1.5 h, the polystyrene(PS)-grafted silica particles were washed with toluene by repeated dispersion–centrifugation cycles until no precipitate was detectable in the supernatant solution added into excess methanol. The centrifugation was carried out at 8000 rpm for at least 30 min. The purified silica particles (with the grafted polymer) were freeze-dried from a benzene solution. To cleave the graft polymer from the silica surface, an aliquot of the sample (7.5 mg) was treated with a mixture of 5% aqueous HF solution (3.75 mL) and toluene (3.75 mL) containing trioctylmethylammonium chloride (27 mg) as a phase transfer catalyst.<sup>23</sup> After stirring for 2 h, the organic phase was neutralized by Na<sub>2</sub>CO<sub>3</sub> and subjected to gel permeation chromatographic (GPC) measurement. The GPC analysis revealed that the graft polymer (PS<sub>0</sub>) had a number-average molecular weight  $M_n$  of 3400 and a polydispersity index  $M_w/M_n$  of 1.05. The Fourier transform infrared (FT-IR) absorption analysis of the PS<sub>0</sub>-grafted silica particle enabled us to estimate the amount of grafted polymer and calculate the graft density to be 0.38 chains/nm<sup>2</sup>. This graft density is almost the same as the previously reported value.<sup>18,26</sup>

The dithiobenzoyl group (X group) was introduced as a RAFT moiety at the free chain end of the graft polymer with a Br moiety by dispersing the polymer-grafted silica particles (0.75 g) in 44 mL of degassed toluene solution of CuBr (0.11 g, 0.77 mmol), dHbipy (0.53 g, 1.5 mmol), and PDB (a RAFT agent; 1.1 g, 4.3 mmol) and heating it at 90 °C for 6 h. After the reaction, the silica particles were purified as described above. The ultraviolet–visible (UV–vis) absorption spectroscopy revealed that the silica particles had the absorption band at around 300 nm ascribable to the X group. The intensity of this band indicated that about 70% of the PS<sub>0</sub> graft polymers had an X group at the chain end.

**Kinetic Analysis of RAFT-Mediated Graft Polymerization.** The silica particle grafted with the X-terminated PS<sub>0</sub> (PS<sub>0</sub>–X) was dispersed in styrene by ultrasonication, degassed by several freeze–pump–thaw cycles, and sealed in a glass tube. The concentration of the grafted silica particle was 0.6 wt %. In some cases, PDB (0.011 M) was added to the solution. The polymerization was carried out at 110 °C for various intervals of time. After the polymerization, the silica particles were washed with toluene by repeated dispersion–centrifuga-

tion cycles as described above. The purified silica particles with the grafted polymer were freeze-dried from a benzene solution.

The weight ( $w_g$ ) of the grafted PS relative to that of the silica particles was estimated by FT-IR absorption measurement. The intensity of the absorption band at around  $1480\text{ cm}^{-1}$  due to PS was compared with that at around  $800\text{ cm}^{-1}$  due to silica particle. The relative absorption coefficients of these two bands were determined with an error less than 10% from FT-IR absorption spectra of PS/silica mixtures with various mixing ratios.

The graft polymer cleaved from the particle by the above-mentioned method and the free polymer produced in solution were characterized by GPC.

**Measurements.** GPC measurements were made on a Tosoh high-speed liquid chromatograph, Tosoh Corp., Japan. Sample detection and quantification were made with a Tosoh refractive index detector, RI-8020. Tosoh column systems, G2500HXL + G3000HXL + G4000HXL, used for relatively low-molecular weight (MW) polymers and G3000HXL + G4000HXL + G5000HXL + G6000HXL, used for higher-MW polymers, were calibrated by the standard PSs supplied by Tosoh. The average size of the column beads is  $5\text{ }\mu\text{m}$  for G2500HXL, G3000HXL, and G4000HXL and  $9\text{ }\mu\text{m}$  for G5000HXL and G6000HXL. Tetrahydrofuran was used as eluent, and the flow rate was adjusted to 0.8 and 1.0 mL/min for the lower- and higher-MW column systems, respectively. The column temperature was maintained at  $40\text{ }^\circ\text{C}$ . The FT-IR absorption spectra were recorded using the KBr pellet method on an FTS-6000 FT-IR spectrometer (BioRad Laboratories Inc., USA) equipped with a liquid nitrogen-cooled MCT (MgCdTe) detector. UV-vis absorption spectra were taken on a UV-2200 spectrophotometer (Shimadzu Corp., Japan).

## Results and Discussion

### Polymerization without Added Free RAFT Agent.

The bulk polymerization of styrene dispersed with the  $\text{PS}_0$ -X-grafted silica particles was carried out at  $110\text{ }^\circ\text{C}$  with no free RAFT agent. In this system, thermally produced primary radicals and the PS radicals initiated by them will attack the X group (the RAFT moiety) of the graft polymer, thus initiating graft polymerization. Figure 3 shows the plots of  $M_n$  and  $M_w/M_n$  of the graft (cleaved) and free polymers and the total grafted amount ( $w_g$ ) including the  $\text{PS}_0$  as a function of monomer conversion. Here, the initially inactive graft polymers without X group (ca. 30% of the  $\text{PS}_0$  graft polymers) were also taken into the calculation of  $M_n$  and  $M_w/M_n$  of the graft polymer and  $w_g$ . The  $M_n$  value of the graft polymer increases with increasing conversion at the early stages of polymerization but levels off at conversions higher than ca. 20%, while its  $M_w/M_n$  value is in the range 1.5–3.0. The  $w_g$  value also levels off at about 20% conversion, while the monomer conversion continues to increase to higher values. The figure also suggests that the free polymers have larger  $M_n$  and lower  $M_w/M_n$  as compared with those of the graft polymers.

All these results suggest the following picture of what happens in this system. The primary radicals thermally produced in the bulk styrene phase predominantly attack styrene to produce PS radicals, some of which, before propagating to the full length limited by bimolecular termination and conventional chain transfer reactions, can undergo a RAFT reaction with one of the graft chains, turning to a free dormant chain  $\text{PS-X}$ , i.e., a free PS capped with a RAFT moiety. In this way, the concentration of free  $\text{PS-X}$  would increase with time or conversion, but since the number of the  $\text{PS}_0$ -X chains grafted on the silica particles is much smaller than (less than 10% of) the total number of the polymers (or primary radicals) produced in the bulk phase of styrene

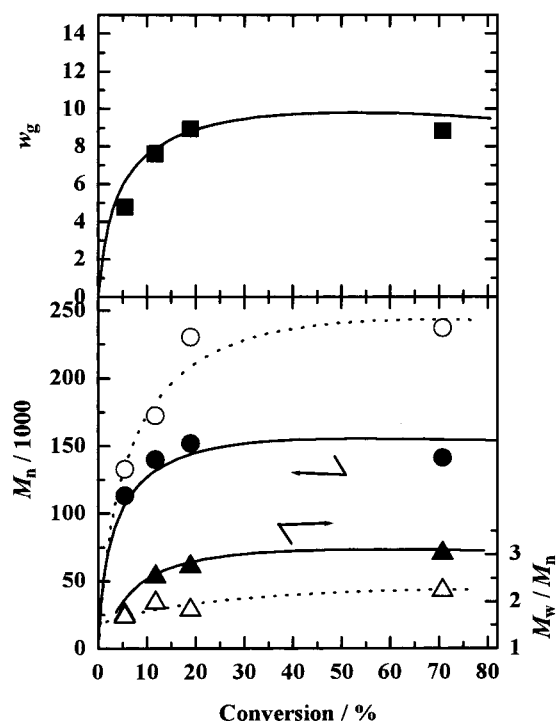


**Figure 3.** Plots of  $M_n$  and  $M_w/M_n$  of the graft (filled symbols) and free (open symbols) polymers and the graft polymer/silica ratio ( $w_g$ ) by weight as a function of monomer conversion ( $110\text{ }^\circ\text{C}$ );  $[\text{PDB}] = 0\text{ M}$ .

during the course of polymerization, the free  $\text{PS-X}$  would have little effect on controlling the polymerization. At the early stages of polymerization, they would mostly remain dormant without being reactivated and hence remain small in molecular weight. After all of the RAFT moieties of the graft chains have moved to the bulk phase, in this way, the system will undergo just conventional thermal polymerization of styrene with a trivial effect of the free  $\text{PS-X}$  chains, yielding large and nearly constant  $M_n$  and  $M_w/M_n$ , as shown in Figure 3. On the other hand, the graft  $\text{PS}_0$ -X chain activated by the free radical would undergo propagation until it makes an exchange (RAFT) reaction with a neighboring graft chain or a bimolecular termination reaction with other graft or free radical. In this way, the dormant graft chains (graft chains with a X group at the end) would slowly increase in molecular weight, i.e., in a controlled fashion. Therefore, at a very early stage of polymerization, the characteristics of the graft and free polymers can be different, as will be discussed later on (cf. Figure 10). However, as the number of dormant graft chains decreases with conversion, the exchange reaction with neighboring dormant graft chains would become less and less likely to occur, and the graft radical would just propagate to a large molecular weight to be terminated predominantly by a free radical in solution (or by a conventional chain transfer).

### Polymerization with Added Free RAFT Agent.

The results given in the last section suggest the importance of adding a free RAFT agent in solution to control the graft as well as free polymerizations. The presence of a sufficient concentration of the RAFT species in the bulk phase would not only control the polymerization in the bulk phase but also effectively maintain the concentration of dormant graft chains by the exchange reaction of a graft radical with a dormant



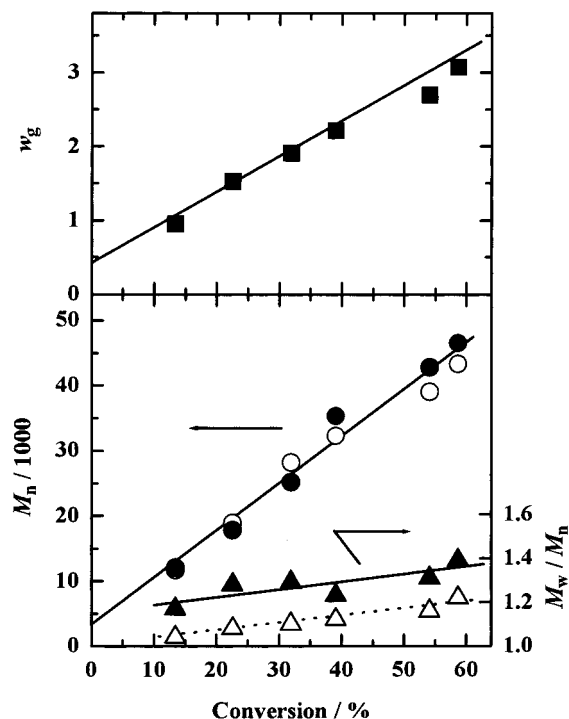


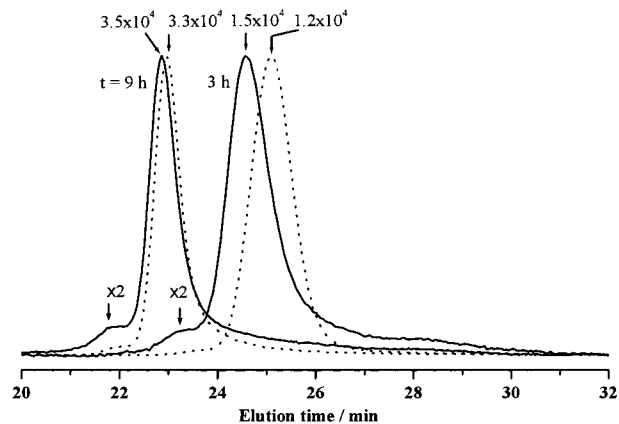
**Figure 4.** Plots of  $M_n$  and  $M_w/M_n$  of the graft (filled symbols) and free (open symbols) polymers and the graft polymer/silica ratio ( $w_g$ ) by weight as a function of monomer conversion (110 °C); [PDB] = 0.011 M.

free chain, thus keeping the graft polymerization under control even at high conversions. For this reason, the polymerization of styrene with  $PS_0$ -X-grafted silica particles was carried out in the presence of PDB (0.011 M) as a free RAFT agent.

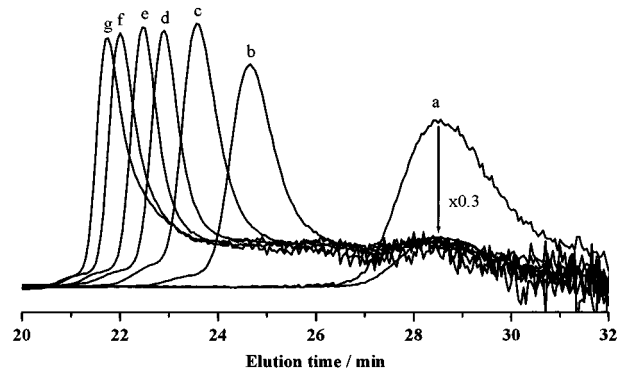
Figure 4 shows the plots of  $M_n$  and  $M_w/M_n$  of the graft (cleaved) and free polymers and the grafted amount  $w_g$  as a function of monomer conversion. This figure indicates the followings: (1) the  $M_n$  of the graft (cleaved) polymer is very close to that of the free polymer, and (2) both are directly proportional to conversion. (3) The  $M_w/M_n$  is remarkably small in all cases, but (4) the  $M_w/M_n$  of the graft polymer is systematically larger than that of the free polymer. These results clearly show that the addition of the free RAFT agent had the expected effect of controlling the graft as well as free polymerizations. However, result 4 needs interpretation.

Figure 5 shows examples of the GPC curves of the graft (cleaved) and free polymers. The difference in peak molecular weight ( $M_p$ ) between the graft (cleaved) and free polymers is nearly equal to the  $M_n$  (3400) of  $PS_0$ , meaning that the two polymers had nearly the same increase in molecular weight. At the elution time corresponding to the doubled  $M_p$ , a shoulder is observed for both graft polymers. This was the case with all the graft (cleaved) polymers prepared via the RAFT process, and the shoulder may be assignable to dead chains produced by recombination of polymer radicals. On the other hand, no such shoulder is detectable in the GPC curves of the free polymers (the broken curves in Figure 5). This means that recombination occurs much more frequently on the surface than in solution.

The GPC data are replotted in Figure 6 where the ordinate scale is the number density of the polymers with the total area under the curve normalized to a constant value. This plot clearly reveals that about 30%



**Figure 5.** GPC curves for the graft (solid curve) and free (broken curve) polymers at 3 and 9 h of polymerization at 110 °C; [PDB] = 0.011 M. The lower-MW column system was used.



**Figure 6.** GPC curves for the graft polymers before (a) and after the RAFT polymerization for (b) 3, (c) 6, (d) 9, (e) 12, (f) 18, and (g) 24 h; [PDB] = 0.011 M. The lower-MW column system was used. The ordinate scale is the number density of the polymers with the total area under the curve normalized to a constant value.

of the original graft polymer is inactive and remains at the original elution times without growth, as expected from about 70% transformation of the terminal halogen atom of the  $PS_0$  to the X group. This is one of the reasons why the  $M_w/M_n$  ratio of the graft polymer is always somewhat larger than that of the free polymer (see Figure 4). As the polymerization proceeds, the sharp peak moves to the higher-molecular-weight (MW) side, leaving a long tail or plateau reaching the original elution times. Namely, as polymerization time increases, the plateau extends to a higher-MW region, but the lower-MW region of the plateau remains unchanged. This clearly indicates that the plateau is ascribed to dead chains. Remembering the existence of a shoulder at the highest MW region of the elution curves (Figure 5), we may reasonably conclude that these dead  $PS$  chains were produced predominantly by recombination. All these considerations suggest that the graft (cleaved) polymer consists of three main components, which are (a) potentially active (dormant) chains, (b) recombined (dead) chains, and (c) originally inactive precursory chains. To evaluate the fractions of the individual components, the GPC curve was divided into the three components as illustrated in Figure 7. By assuming that all the dead chains (component b) were produced by recombination of graft radicals, the surface density,  $\sigma_d$ , of the dormant chains (component a) was evaluated as a function of time, which is shown in Figure 8. The error

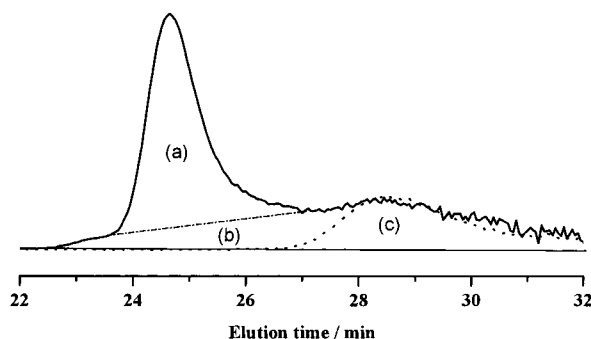


**Figure 7.** Division of the GPC curve into three components of graft polymers: (a) potentially active (dormant) graft chain, (b) recombined graft chain, and (c) initially inactive graft chain.

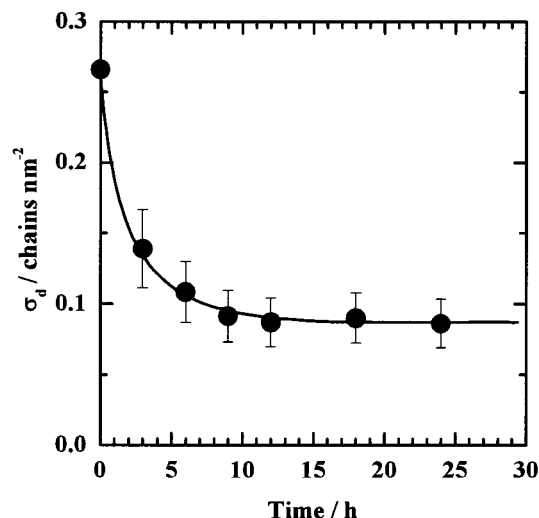


**Figure 8.** Time dependence of the surface density,  $\sigma_d$ , of the dormant (potentially active) graft chains.

bars in the figure represent a possible estimation error, which mainly comes from the ambiguity of the boundary between the components a and b. The figure shows that  $\sigma_d$  decreases with polymerization time sharply at first and then slowly, reaching about 0.08 chains/nm<sup>2</sup> at a later stage of polymerization. This means that in this RAFT system the termination reaction occurs with a surprisingly high rate at an early stage, where  $\sigma_d$  is large, while virtually no termination occurs after  $\sigma_d$  reaches about 0.08 chains/nm<sup>2</sup>. Comparison of parts f and g of Figure 6 clearly shows that the MW of the shoulder does not increase after 18 h while that of the peak increases, confirming the above-mentioned suppression of termination at a later stage of polymerization.

A possible reason for the enhanced recombination observed on the surface might be a higher local concentration of radicals on the surface than in solution. To check this, we compared the GPC curve of the graft polymer prepared by the RAFT process with that prepared by the ATRP one. A PS was grafted on silica particle by the surface-initiated ATRP under the condition where the concentration of the graft radical was similar to that for the RAFT system. Figure 9 shows an example of the GPC curve of the graft polymer produced by the ATRP process. No such clear shoulder as was observed for the RAFT system is seen at around the doubled  $M_p$  indicated by the arrow in the figure, suggesting that the recombination on the surface is insignificant in the ATRP system. Therefore, a high

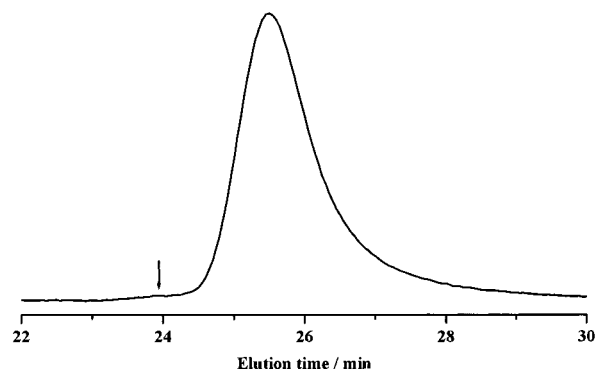


**Figure 9.** GPC curve of the graft polymer produced by the ATRP process at 110 °C. The lower-MW column system was used.

surface concentration of the graft radical alone cannot explain the enhanced recombination.

As another possibility, one might argue that the recombination rate on the surface depends not only on the radical concentration but also on the frequency of graft-radical formation. Analogously to the static fluorescence quenching (e.g., in a rigid matrix) in the field of photophysics,<sup>30</sup> the “active sphere” model may be applicable; i.e., a graft radical formed on the surface will be assumed to recombine with a 100% efficiency when and only when a graft radical exits within an active sphere, the radius of which is independent of the lifetime of a graft radical. In this extreme case, the recombination rate on the surface should be proportional to the frequency of graft-radical formation under the condition of a constant graft-radical concentration. The frequency ( $p_a$ ) of a dormant graft chain to be activated by a free (unbound) radical or activator is given by the following equations:

$$p_a = k_{ex}[P_f^*] \quad (\text{RAFT system}) \quad (1)$$

$$p_a = k_A[\text{CuBr}] \quad (\text{ATRP system}) \quad (2)$$

where  $[P_f^*]$  is the concentration of free radical, and  $k_{ex}$  and  $k_A$  are the rate constants of degenerative (exchange) chain transfer and CuBr-catalyzed activation, respectively. From the literature values of  $k_{ex}$ <sup>31</sup> and  $k_A$ ,<sup>32</sup> the  $p_a$  value was estimated to be 0.028 s<sup>-1</sup> for the RAFT system and 0.018 s<sup>-1</sup> for the ATRP system. Such a small difference cannot explain the observed large difference in the recombination frequency between the two systems.

We therefore conclude that the enhanced recombination is specific to the RAFT-mediated graft polymerization and is due to the migration of radical on the surface by sequential chain transfer reactions. By this “reaction–diffusion” mechanism, two active radicals originally far apart from each other can come closer after many steps of the exchange reactions. The frequency of the exchange reactions should primarily depend on the density,  $\sigma_d$ , of the dormant graft chains. When  $\sigma_d$  is large, the surface radical can migrate or diffuse rapidly, hence the high rate of termination. There should be a critical surface density below which virtually no exchange reaction possibly occurs. This critical value of  $\sigma_d$  should be a function of the chain length of the dormant graft chain. The  $\sigma_d$  value of about 0.08 chains/nm<sup>2</sup> suggested above (cf. Figure 8) may be the critical density of the present system.

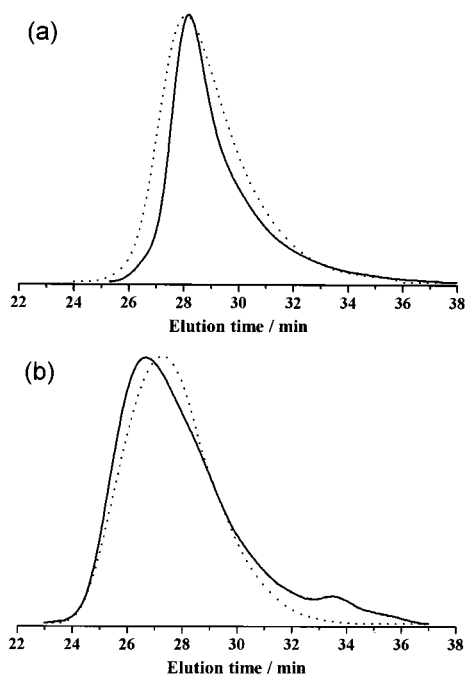


**Figure 10.** GPC curves for graft (solid curves) and free (broken curves) polymers at (a) 2 h and (b) 7 h of polymerization (about 6% and 19% of conversions, respectively) at 110 °C with no free RAFT agent added. The higher-MW column system was used.

Another piece of evidence for frequent chain transfer reactions occurring among graft chains can be found in the experimental data for an early stage of the RAFT-mediated graft polymerization with no added free RAFT agent. In Figure 10, the GPC curves of the graft (cleaved) polymers are compared with those of the free polymers. At a low conversion (ca. 6%), the former GPC curve is characterized by a narrower peak and a longer tail than the latter one, while the  $M_w/M_n$  values of the graft and free polymers are nearly the same (cf. Figure 3). The more prominent lower-MW tail of the graft polymer may be ascribed to the enhanced termination between graft radicals. The narrower peak means that the graft polymer which escaped from termination has narrower MW distribution, indicating that more frequent chain transfer reactions occur on the surface than in the solution (for a frequency vs polydispersity index relation, see ref 33). In later stages of polymerization, most graft chains are terminated, and this effect becomes unclear. Indeed, the GPC peak of the graft polymer became broader in later stages, being very close to that of the free polymer. Because of the more prominent low-MW tail, the  $M_w/M_n$  value of the graft polymer was larger than that of the free polymer.

## Conclusions

In a RAFT-mediated graft polymerization, a very effective surface migration of the graft radical can occur via successive degenerative (exchange) chain transfer reactions if the surface density  $\sigma_d$  of the dormant (potentially active) graft chain is high enough. This effective surface migration narrows the chain length distribution of the graft chains. At the same time, however, the surface migration allows the graft radicals to undergo bimolecular termination at an unusually high rate, especially when  $\sigma_d$  is large, which broadens the chain length distribution. There is a critical value of  $\sigma_d$  below which the surface migration of the graft

radicals hardly occurs. For graft densities below this limit, a RAFT system would behave similarly to, for example, an ATRP system.

**Acknowledgment.** This work was supported in part by a Grant-in-Aid for Scientific Research (Grant-in-Aid 12450385) to T.F. from the Ministry of Education, Culture, Sports, Science and Technology, Japan, and by Industrial Technology Research Grant Program in 2000 to Y.T. from the New Energy and Industrial Technology Development Organization (NEDO) of Japan.

## References and Notes

- (1) Solomon, D. H.; Rizzardo, E.; Cacioli, P. *Eur. Pat. Appl.* EP135280 (*Chem. Abstr.* **1985**, *102*, 221335q).
- (2) Georges, M. K.; Veregin, R. P. N.; Kazmaier, P. M.; Hamer, G. K. *Macromolecules* **1993**, *26*, 2987.
- (3) Hawker, C. J. *J. Am. Chem. Soc.* **1994**, *116*, 11185.
- (4) Greszta, D.; Matyjaszewski, K. *Macromolecules* **1994**, *27*, 638.
- (5) Catala, J.-M.; Bubel, F.; Hammouch, S. O. *Macromolecules* **1995**, *28*, 8441.
- (6) (a) Fukuda, T.; Terauchi, T.; Goto, A.; Tsujii, Y.; Miyamoto, T.; Shimizu, Y. *Macromolecules* **1996**, *29*, 3050. (b) Fukuda, T.; Terauchi, T.; Goto, A.; Ohno, K.; Tsujii, Y.; Miyamoto, T.; Kobatake, S.; Yamada, B. *Macromolecules* **1996**, *29*, 6393.
- (7) (a) Benoit, D.; Chaplinski, V.; Braslau, R.; Hawker, C. J. *J. Am. Chem. Soc.* **1999**, *121*, 3904. (b) Benoit, D.; Grimaldi, S.; Robin, S.; Finet, J. P.; Tordo, P.; Gnanou, Y. *J. Am. Chem. Soc.* **2000**, *122*, 5929.
- (8) (a) Kato, M.; Kamigaito, M.; Sawamoto, M.; Higashimura, T. *Macromolecules* **1995**, *28*, 1721. (b) Sawamoto, M.; Kamigaito, M. *CHEMTECH* **1999**, *9*, 30.
- (9) (a) Wang, J.-S.; Matyjaszewski, K. *J. Am. Chem. Soc.* **1995**, *117*, 5614. (d) Matyjaszewski, K. *Chem. Eur. J.* **1999**, *5*, 3095.
- (10) Percec, V.; Barboiu, B. *Macromolecules* **1995**, *28*, 7970.
- (11) Granel, C.; Dubois, Ph.; Jérôme, R.; Teyssié, Ph. *Macromolecules* **1996**, *29*, 8576.
- (12) Haddleton, D. M.; Jasieczek, C. B.; Hannon, M. J.; Scooter, A. J. *Macromolecules* **1997**, *30*, 2190.
- (13) Le, T. P. T.; Moad, G.; Rizzardo, E.; Thang, S. H. *International Pat. Appl. PCT/US97/12540*, WO9801478 (*Chem. Abstr.* **1998**, *128*, 115390).
- (14) Rizzardo, E.; Chiefari, J.; Chong, B. Y. K.; Ercole, F.; Krstina, J.; Jeffery, J.; Le, T. P. T.; Mayadunne, R. T. A.; Meijs, G. F.; Moad, C. L.; Moad, G.; Thang, S. H. *Macromol. Symp.* **1999**, *143*, 291.
- (15) Destarac, M.; Charmot, D.; Franck, X.; Zard, X. Z. *Macromol. Rapid Commun.* **2000**, *21*, 1035.
- (16) (a) Tsavalas, J. G.; Schork, F. J.; de Brouwer, H.; Monteiro, M. J. *Macromolecules* **2001**, *34*, 3938. (b) Monteiro, M. J.; de Barbeyrac, J. *Macromolecules* **2001**, *34*, 4416.
- (17) Matyjaszewski, K., Ed.; *ACS Symp. Ser.* **1998**, *685*; **2000**, 768.
- (18) (a) Ejaz, M.; Yamamoto, S.; Ohno, K.; Tsujii, Y.; Fukuda, T. *Macromolecules* **1998**, *31*, 5934. (b) Ejaz, M.; Ohno, K.; Tsujii, Y.; Matsumoto, M.; Fukuda, T. *Macromolecules* **2000**, *33*, 2870. (c) Ejaz, M.; Tsujii, Y.; Fukuda, T. *Polymer* **2001**, *42*, 6811.
- (19) Huang, X.; Wirth, M. J. *Macromolecules* **1999**, *32*, 1694.
- (20) (a) Zhao, B.; Brittain, W. J. *J. Am. Chem. Soc.* **1999**, *121*, 3557. (b) Zhao, B.; Brittain, W. J.; Zhou, W.; Cheng, S. Z. D. *J. Am. Chem. Soc.* **2000**, *122*, 2407.
- (21) (a) Hussemann, M.; Malmström, E. E.; McNamara, M.; Mate, M.; Mecerreyes, D.; Benoit, D. G.; Hedrick, J. L.; Mansky, P.; Huang, E.; Russell, T. P.; Hawker, C. J. *Macromolecules* **1999**, *32*, 1424. (b) Husemann, M.; Morrison, M.; Benoit, D.; Frommer, J.; Mate, C. M.; Hinsberg, W. D.; Hedrick, J. L.; Hawker, C. J. *J. Am. Chem. Soc.* **2000**, *122*, 1844.
- (22) Matyjaszewski, K.; Miller, P. J.; Shukla, N.; Immaraporn, B.; Gelman, A.; Luokala, B. B.; Siclován, T. M.; Kickelbick, G.; Vallant, T.; Hoffmann, H.; Pakula, T. *Macromolecules* **1999**, *32*, 8716.
- (23) (a) von Werne, T.; Patten, T. E. *J. Am. Chem. Soc.* **1999**, *121*, 7409. (b) von Werne, T.; Patten, T. E. *J. Am. Chem. Soc.* **2001**, *123*, 7497.
- (24) de Boer, B.; Simon, H. K.; Werts, M. P. L.; van der Vegte, E. W.; Hadziioannou, G. *Macromolecules* **2000**, *33*, 349.
- (25) Kim, J.-B.; Bruening, M. L.; Baker, G. L. *J. Am. Chem. Soc.* **2000**, *122*, 7616.

- (26) (a) Yamamoto, S.; Ejaz, M.; Tsujii, Y.; Matsumoto, M.; Fukuda, T. *Macromolecules* **2000**, *33*, 5602. (b) Yamamoto, S.; Ejaz, M.; Tsujii, Y.; Fukuda, T. *Macromolecules* **2000**, *33*, 5608.
- (27) (a) Yamamoto, S.; Tsujii, Y.; Fukuda, T. *Macromolecules* **2000**, *33*, 5995.
- (28) Pakula, T. *Macromol. Symp.* **1999**, *139*, 49.
- (29) Matyjaszewski, K.; Patten, T. E.; Xia, J. *J. Am. Chem. Soc.* **1997**, *119*, 674.
- (30) Perrin, F. *C. R. Acad. Sci. Paris* **1924**, *178*, 1978.
- (31) Goto, A.; Sato, K.; Tsujii, Y.; Fukuda, T.; Moad, G.; Rizzardo, E.; Thang, S. H. *Macromolecules* **2001**, *34*, 402.
- (32) Ohno, K.; Goto, A.; Fukuda, T.; Xia, J.; Matyjaszewski, K. *Macromolecules* **1998**, *31*, 2699.
- (33) Fukuda, T.; Goto, A. *Macromol. Rapid Commun.* **2000**, *21*, 151.

MA010733J